Regulation of a Drosophila cGMP-PDE by prenylation and interaction with a prenyl-binding protein

Jonathan P Day, Vaughn Cleghon, Miles Douglas Houslay, Shireen A. Davies

Regulation of a *Drosophila* cGMP-PDE by prenylation and interaction with a prenyl-binding protein

Jonathan P. DAY, Vaughn CLEGHON[1], Miles D. HOUSLAY[2]* and Shireen-A. DAVIES

Institute of Biomedical and Life Sciences, Divisions of Molecular Genetics, University of Glasgow, Glasgow G11 6NU, U.K, [1]Cincinnati Children's Hospital Medical Center, Division of Developmental Biology, 3333 Burnet Ave, Cincinnati, Ohio 45229, [2]Institute of Biomedical and Life Sciences, Division of Biochemistry and Molecular Biology, University of Glasgow, Glasgow G12 8QQ, U.K

*To whom correspondence should be addressed (email m.houslay@bio.gla.ac.uk)

Running head: Prenylation of cGMP-PDE in *Drosophila*

Post-translational modification by isoprenylation is a pivotal process for the correct functioning of many signalling proteins. The *Drosophila melanogaster* cGMP-specific phosphodiesterase, *Dm*PDE5/6, possesses a C*aa*X-box prenylation signal-motif, as do several novel cGMP-PDEs from insect and echinoid species. *Dm*PDE5/6 is prenylated *in vivo* at Cys1128 and is localised to the plasma membrane when expressed in *Drosophila* S2 cells. Site-directed mutagenesis of the prenylated cysteine residue (C1128S-*Dm*PDE5/6), pharmacological inhibition of prenylation or co-expression of the *Drosophila* prenyl-binding protein, *Dm*PrBP/δ, each alters the sub-cellular localisation of *Dm*PDE5/6. Thus prenylation constitutes a critical post-translational modification of *Dm*PDE5/6 for membrane-targeting. Co-immunoprecipitation and sub-cellular fractionation experiments show that *Dm*PDE5/6 interacts with *Dm*PrBP/δ in *Drosophila* S2 cells. Transgenic lines allow targeted expression of tagged, prenylation deficient C1128S-*Dm*PDE5/6 to Type I (principal) cells in *Drosophila* Malpighian tubules, an *in vivo* model for *Dm*PDE5/6 function. In contrast to wild-type *Dm*PDE5/6, which was exclusively associated with the apical membrane, the C1128S-*Dm*PDE5/6 mutant form was located primarily in the cytosol, although some residual association occurred at the apical membrane. Despite the profound change in intracellular localisation of C1128S-*Dm*PDE5/6, active transport of cGMP is affected the same as by *Dm*PDE5/6. This suggests that in addition to prenylation and interaction with *Dm*PrBP/δ, further functional membrane-targeting signals exist within *Dm*PDE5/6.

Keywords: renal epithelium, *Drosophila* cGMP, PDE6, PDE5, prenylation, S2 cell

INTRODUCTION

The precise sub-cellular localisation of components of cell signalling networks which allows the spatio-temporal control of signalling is of major importance in biology [1, 2]. This is exemplified by signalling systems employing the cyclic nucleotides cAMP and cGMP. The local concentrations of cyclic nucleotides is controlled by the precise positioning within the cell of cyclases, that catalyse their formation [3, 4], and cyclic nucleotide phosphodiesterases (PDEs) that catalyse their degradation [5, 6]. Indeed, it has been shown recently that PDEs can be tethered to sub-cellular targets by exquisitely precise interactions [7, 8]. The result is tight control of cyclic nucleotide regulated effector molecules such as cAMP or cGMP-dependent protein kinases [8-10]. Therefore, the sub-cellular localization of PDEs has fundamental consequences for cellular physiology.

Many of the proteins involved in signal transduction events undergo some form of post-translational lipid modification essential for their correct localisation and function, including N-terminal myristoylation and C-terminal isoprenylation and palmitoylation [11, 12]. Proteins are traditionally thought to undergo

isoprenylation at a consensus C-terminal C*aa*X-box motif, where *a* is an aliphatic residue and X is any residue [13]. However, recent analysis suggests that certain, non-aliphatic residues can exist at position +1 after the conserved cysteine and that there is a clear preference for hydrophobic residues at position +3 [14]. Isoprenylation is thought to be an important mediator of protein-membrane interactions. For example, ablation of prenylation in the H-, N- and K-Ras GTPase family, completely redistributes these membrane-bound proteins to the cytosol [15].

The mammalian, retinal cGMP-specific phosphodiesterase (PDE6) has been shown to undergo C-terminal isoprenylation at its alpha, beta and alpha' catalytic subunits [16-18]. The PDE6 alpha and alpha' subunits are modified by farnesyl lipids, whereas the beta subunit is modified by the addition of geranylgeranyl groups. Such modifications are apparently required for binding of these PDEs to rod outer segment membranes [18]. Several prenylated proteins including retinal PDE6 catalytic subunits, rhodopsin kinase (GRK1), and the small GTPases Ha-Ras and Rap, have been shown to bind to the prenyl binding protein (PrBP/δ), formerly PDEδ, [19-21]. PrBP/δ participates in the transport of PDE6 catalytic subunits and GRK1 from the ER, where prenylation occurs, to photoreceptor outer segments [22].

In the genetic model organism, *Drosophila melanogaster*, a close sequence and functional homologue of both vertebrate PDE5 [23] and PDE6 [24], *Dm*PDE5/6, has been identified [25]. *Dm*PDE5/6 is a high K_m enzyme that specifically hydrolyses cGMP and is sensitive to the PDE5-selective inhibitors, sildenafil and zaprinast [26, 27]. *Dm*PDE5/6 also contains a C-terminal C*aa*X-box prenylation motif [25]. In *Drosophila*, endogenous *Dm*PDE5/6 expression has been documented in head and body [25]; as well as in the Malpighian (renal) tubule [28], a cGMP-modulated transporting epithelium that is critical for detoxification, osmoregulation and immunity. Recent work has demonstrated a novel role in the modulation of cGMP efflux by *Dm*PDE5/6 in tubule [28].

Drosophila transgenics [29] allow a sophisticated system for ectopic over-expression or ablation of genes of choice in particular cell-types or tissues in the intact animal. Thus, the tubule provides a powerful *in vivo* model in which to assess regulation and function of novel cG-PDEs. We show that *Dm*PDE5/6 is a prenylated enzyme which is a member of a family of PDE5-like enzymes with prenylation motifs. We also show that *Dm*PDE5/6 can associate with *Drosophila* prenyl binding protein (*Dm*PrBP/δ), and show that the localisation of *Dm*PDE5/6 in the tubule is altered when its prenylation is ablated.

MATERIALS AND METHODS

Bioinformatics

The amino acid sequences of *Drosophila melanogaster* PDE5/6 (*Dm*PDE5/6 encoded by gene *CG8279*) homologues were identified by BLAST-searching the non-redundant peptide sequence database using *Dm*PDE5/6 as the query sequence. Retrieved sequences were individually examined for the presence of putative C*aa*X-box prenylation motifs. Those sequences containing such motifs were subjected to further analysis using the PrePS prenylation prediction suite (http://mendel.imp.ac.at/sat/PrePS/index.html) [14]. Accession numbers of sequences were as follows: *Drosophila pseudoobscura* GA20950-XP_001358768, *Anopheles gambiae* AGAP004119-XP_312997, *Apis mellifera* XP_394107, *Triboleum castaneum* XP_967847, *Strongylocentrotus pupuratus* PDE5a-NP_001029121, *Danio rerio* XP_697567, *Xenopus tropicalis* PDE5a-NP_001072812, *Homo sapiens* PDE6A-P16499, *Homo sapiens* PDE6B-NP_000274, *Homo sapiens* PDE6C-P51160, *Homo sapiens* PDE5A1-NP_001074.2, *Homo sapiens* PDE11A4-NP_058649.3, *Drosophila melanogaster* Ras85D-NP_476699. Alignment of the C-terminal 25 amino acids of selected proteins and sequence similarity trees were made using ClustalW (http://www.ebi.ac.uk/clustalw/), and drawn using BioEdit (http://www.mbio.ncsu.edu/BioEdit/bioedit.html).

*Dm*PrBP/δ (encoded by gene *CG9296*) was identified from Flybase, (http://flybase.bio.indiana.edu/.bin/fbidq.html?FBgn0032059).

Site-directed mutagenesis of PDE6. Targeted PCR mutagenesis of *Dm*PDE5/6 cysteine 1128 to serine (to achieve *Dm*PDE5/6 C1128S) was performed according to a commercial mutagenesis protocol (Stratagene). The *Dm*PDE5/6 (*CG8279*) plasmid template was PCR amplified using primers (Suppl.

Table 1) designed to achieve the TGC to AGC mutation, and to include complementary flanking sequences of 20 bp. Purified PCR products were digested with DpnI to remove template DNA, and 2 µl of the digest was used to transform chemically competent DH5α cells.

Expression of *Dm*PDE5/6 in Sf9 cells

Recombinant baculovirus generation utilised the BaculoGold system (BD PharMingen). The open reading frames encoding wild-type *Dm*PDE5/6 and *Dm*PDE5/6 C1128S, tagged at the N-terminus with a V5-epitope, were cloned into the baculovirus transfer vector pVL1393 (BD PharMingen) using the BamHI and NotI restriction sites, and plasmids purified. For all infections, a P2 recombinant viral stock, generated after two rounds of amplification via standard methods was used. For protein expression, 5 x 10^6 Sf9 cells at exponential growth were plated into 75 cm^2 cell culture flasks in 9 ml of medium. 0.5 ml of P2 viral stock was added and cells were incubated at 27°C for 36 h. Cells were harvested by centrifugation at 2,000 g for 5 min, the supernatant discarded and the cell pellet was used either for labelling experiments or for PDE assays.

***In vitro* prenylation experiments**

Three aliquots of 5 x 10^6 Sf9 cells were plated into 75 cm^2 cell culture flasks in 10 ml of media and allowed to adhere for 30 min before addition of 0.5 ml of recombinant viral stock.

Infection was allowed to proceed for 24 hours before addition of Mevinolin (Sigma) (40 µmol/l) for 1 h, after which cells were centrifuged and resuspended in 2 ml of medium. Cells were then incubated for 16 h in 25 µCi ml^{-1} [5-^{3}H] mevalonic acid (39 Ci/mmol, Sigma) and then harvested, washed once in PBS, and pelleted by centrifugation at 1,500 g for 2 min. The pellet was lysed in 200 µl of 3T3 lysis buffer (25 mM HEPES, pH 7.4, 50 mM NaCl, 10% glycerol, 1% Triton X100) and the protein concentration measured. 70 µg of protein was removed for Western analysis and *Dm*PDE5/6 was immunoprecipitated from the remaining protein sample with purified polyclonal anti-*Dm*PDE5/6 antibody using standard procedures [25]. The protein A beads were boiled in 10 µl of SDS loading buffer and used to load two 10 % SDS PAGE gels. One gel was run for Western analysis and loaded with 10 µg of total protein, or 3 µl of immunoprecipitated protein sample per lane; and the other was used for fluorography and loaded with 60 µg of total protein and the remainder (20 µl) of the precipitated protein per lane. The gel for fluorography was treated with Enlight (Mo Bi Tec Molecular BioTechnology) for 1 h, dried and fluorographed at -70°C for 1 – 4 weeks. The gel for Western blotting was processed as described below.

Cloning and expression of *Dm*PDE5/6, *Dm*PDE5/6 C1128S, *Dm*Ras85D and *Dm*PrBP/δ in *Drosophila* S2 cells

In order to generate V5-epitope tagged proteins, *Dm*PDE5/6 cloned as described in [25] and *Dm*PrBP/δ were cloned into the S2 vector, pMT/V5-HIS-TOPO (Invitrogen). For cloning of *Drosophila* Ras85D, the Ras85D gene was amplified from an EST (RE53955) obtained from the Berkeley *Drosophila* Genome Project (BDGP, http://www.fruitfly.org/EST/index.shtml) using forward primer (incorporating a BglII restriction site) and reverse primer (incorporating a NotI restriction site). In order to generate GFP-tagged Ras85D, the coding sequence for enhanced green fluorescent protein was PCR-amplified (forward primer: incorporating a BamHI restriction site and optimal Kozak sequence (ACCATGG); reverse primer: incorporating a BamHI restriction site), digested and cloned at the 5' end of Ras85D using the BglII restriction site. The resulting construct was cloned into pMT/V5-HIS-TOPO vector. The open reading frame of *Dm*PrBP/δ was PCR amplified from genomic DNA template using a reverse primer omitting the stop codon, and directly cloned into pMT/V5-HIS-TOPO (Invitrogen). For co-localisation of *Dm*PDE5/6 with *Dm*PrBP/δ a pMT GFP:*Dm*PDE5/6 was generated by inserting the EGFP coding sequence at the 5' end of the *Dm*PDE5/6 open reading frame. These plasmids were then used for the transient transfection of S2 cells under conditions of Cu^{2+}-inducible expression. Cells were cultured according to standard protocols [30]. Approximately 3 x 10^6 cells were used in each transfection, performed using Cellfectin (Invitrogen); transfection efficiencies were routinely 10-25%.

Fractionation experiments

Cellular fractionation was carried out on approximately 3 x 10^6 transiently transfected S2 cells. After harvesting and washing, cells were lysed by incubation on ice for 10 min in 80 µl ice-cold hypotonic buffer (10 mM Tris-HCl pH 7.5, 5 mM $MgCl_2$, 1mM DTT, 1:100 dilution of protease inhibitor cocktail (Sigma)) and then passed through a fine gauge needle 10 times. The homogenate was then adjusted to 0.2 M sucrose by addition of a 1/10^{th} volume of 2 M sucrose solution and subjected to 10 min centrifugation at 1,000 g at 4 ^oC. The pellet was retained as the P1 fraction, and supernatant removed to a fresh tube and centrifuged for 10 min at 15,000g at 4 ^oC. The resulting pellet was retained as the P15 fraction, and supernatant removed to a fresh tube and centrifuged for 30 min at 100,000 g at 4 ^oC to yield the P100 fraction. The supernatant was retained as the S100 fraction. Pellets were washed once in sucrose buffer and resuspended in 88 µl detergent buffer (50 mM Tris-HCl, 2% IGEPAL (Sigma), pH 7.5) and 20 µl each of supernatant and resuspended pellets were analysed by Western blotting.

Western blotting

Tubule or cell samples were homogenised, on ice, in 3T3 lysis buffer with protease inhibitor cocktail (Sigma). Typically, 20 µg of protein samples were separated using SDS PAGE, on 10% gels. Western blotting was carried out using the ECL™ Western Blotting analysis system (Amersham Pharmacia) according to standard protocols using either a 1:5000 dilution of anti-V5 antibody (Invitrogen) followed by a 1:5000 dilution of anti-mouse secondary antibody (Amersham BioSciences) [31] ; or using a monoclonal anti-GFP antibody (Zymed) at 1:1000 dilution.

Immunocytochemistry and confocal microscopy

Immunocytochemistry of S2 cells was carried out according to standard protocols [31] using cells immobilised on poly-L-lysine coated coverslips. Samples were processed and treated with a 1: 1000 dilution of anti-V5 primary antibody (Invitrogen), with secondary staining using anti-mouse FITC, 1:500 (Jackson Laboratories) or anti-mouse Texas Red, 1:500 (AbCam). Cell nuclei were stained with DAPI (4', 6'-diamidino-2-phenylindole hydrochloride) at 1 µg/ml. The coverslips to which samples were attached were then mounted on slides using Vectashield mounting medium (Vector Laboratories) and sealed with glycerol-gelatin.

Tubules expressing GFP:*Dm*PDE5/6 or GFP:C1128S-*Dm*PDE5/6 in principal cells were dissected in Schneider's medium and mounted on poly-L-lysine coated slides. Tubules were fixed and permeabilised as previously described [32] and incubated for 1 h in 1 mg/ml Texas Red-conjugated phalloidin (Sigma)- an F-actin stain indicative of tubule apical membrane [33]- in Phosphate-buffered saline/ 0.3 % v/v Triton. After washing, tubules were DAPI-stained as above. Slides were mounted in Vectashield. Samples were imaged using a Zeiss 510 Meta coupled to an inverted Zeiss microscope using a 405 nm Diode laser / 420-480 nm band pass filter for DAPI, HeNe1 543 nm laser / 561-754 nm band pass filter for Texas Red, and an Argon 488 nm laser / 505-550 nm band pass filter for FITC.

Generation of transgenic lines

The sequence for C1128S-*Dm*PDE5/6 was sub-cloned into *pPmt* vector [34] and used to transform *Drosophila* embryos according to standard techniques as previously described [35]. This allows chromosomal insertion of a UAS-GFP:C1128S-*Dm*PDE5/6 transgene in transformed embryos.

***Drosophila* stocks**

All strains were maintained on standard *Drosophila* diet at 25^oC and 55% humidity, on a 12:12 photoperiod. *Drosophila* lines used in this study were: w^{1118} (parental strain used for transformation of embryos); UAS-GFP:*Dm*PDE5/6 (allows targeted expression of GFP-tagged *DmPDE5/6*, [28]); UAS-GFP:C1128S-*Dm*PDE5/6 (transgenic lines generated for this study, allows targeted expression of GFP-tagged *Dm*PDE5/6 C1128S); c42: GAL4 enhancer trap line, used to drive expression of *UAS* constructs in

only tubule principal cells [35, 36]. The following lines were also used, which were the progeny of crosses between c42 and specific UAS transgenic lines: c42/UAS-GFP:*Dm*PDE5/6; c42/UAS-GFP:C1128S-*Dm*PDE5/6. Adults were used at 7 days post-emergence for all experiments.

cG-PDE assays

Assays for cG-PDE in tubules were performed as previously described [25, 37] using 200 tubules (~40 µg protein) for each sample, homogenised and assayed in 37 MBq/ml tritiated cGMP or cAMP (Amersham Biosciences) in 50 µl KHEM buffer (50 mM KCl, 10 mM EGTA, 1.92 mM $MgCl_2$, 1 mM dithiothreitol (DTT), 50 mM HEPES, pH 7.4, 1 µl Sigma P8340 protease inhibitor cocktail). A final substrate concentration of 10 µM cGMP was used in tubule reactions, as endogenous *Drosophila* cG-PDEs are high K_m enzymes [25]. K_m and relative V_{max} values of *Dm*PDE5/6 and C1128S-*Dm*PDE5/6 expressed in Sf9 cells were determined by carrying out western analysis of lysates and adjusting the amount of protein used so that equal amounts of *Dm*PDE5/6 was added to each cG-PDE reaction. cG-PDE assays were carried out on these samples at 1, 2, 5, 10, 20, 50 and 100 µM cGMP final substrate concentration. Final PDE activity was expressed as pmol or nmol cGMP hydrolysed per min per mg of protein.

cGMP transport assays

Transport assays were based on methodology for ouabain transport [38] and performed according to previously published protocols [28]. Malpighian tubules from seven day old adult flies were set up as for a standard fluid transport assay, as previously described [25]. Experiments were carried out at 100 µM cGMP in the presence of 0.2 µCi of tritiated cGMP (Amersham BioSciences). Tubules were allowed to secrete for 1 h and diameters of the secreted droplets measured. Secreted droplets, and a 1µl aliquot of each bathing droplet were then removed to Eppendorf tubes containing scintillation fluid. The rate of cGMP transport, in fmol/min, was calculated by using the equation: Rate = S[*substrate*]/B*t*; where *S* = counts in the secreted drop (cpm), *substrate* = cGMP concentration (µM), *B* = counts in the bathing drop (cpm), *t* = time (min). The transport ratio was calculated by dividing the concentration of [^{3}H] cGMP in the secreted droplet by the concentration of [^{3}H] cGMP in the bathing droplet. These experiments were performed on tubules from UAS-GFP:C1128S-*Dm*PDE5/6 and c42/UAS-GFP:C1128S-*Dm*PDE5/6. Data for *Dm*PDE5/6 transgenic tubules published in [28]. Results are expressed as units of either rate of transport (pmol cGMP/min) or transport ratio ± SEM, *N*=12.

Statistics

Where appropriate, statistical significance was assessed using Student's *t*-test for unpaired samples, taking $p<0.05$ as the critical value.

RESULTS

***Dm*PDE5/6 is prenylated at a C-terminal C*aa*X-box**

The intracellular targeting of PDEs underpins the generation of intracellular gradients, pools and sinks for cyclic nucleotides, thus providing a critical factor in the regulation of cyclic nucleotide signalling [8, 9]. In a number of systems, prenylation has been shown to provide an important means of regulating the intracellular distribution of signalling molecules by conferring membrane association [12]. To date, however, the catalytic subunits of mammalian PDE6, which are found exclusively in the visual system [39], provide the only PDE for which prenylation has been demonstrated. However, the C-terminus of *Dm*PDE5/6 contains a C*aa*X-box motif of a form such that might be predicted to be modified by the addition of an isoprenyl lipid (Figure 1A and [25]).

We also investigated the possibility that other non-retinal cGMP-PDEs might have C*aa*X-box prenylation motifs. Database searches were performed, using *Dm*PDE5/6 as a query sequence. The results from this bioinformatics analysis revealed the presence of several further putative cGMP-PDEs that contain possible C*aa*X-box motifs (Figure 1A). Alignment of these novel sequences with mammalian PDEs showed that they are more closely related to mammalian PDE5 or PDE11 than the retinal PDE

catalytic subunits (Figure 1B and Table 1). We noted that six out of seven of the putative C*aa*X-boxes contained non-consensus sequences, particularly at the +1 and +3 positions with respect to the conserved cysteine (Figure 1A). To investigate whether these sequences could be functional C*aa*X-boxes, each putative PDE was submitted for analysis by the prenylation prediction suite (PrePS, http://mendel.imp.univie.ac.at/sat/PrePS). This analysis suggested that *Dm*PDE5/6, *D. pseudoobscura* GA20950, *A. gambiae* AGAP004119 and *T. castaneum* XP_967847 are likely substrates for geranylgeranyl transferase 1 (GGT1), whereas *A. mellifera* XP_394107 and *S. purpuratus* PDE5a [40] are likely substrates for farnesyl transferase (FT) (Table 1). The novel putative vertebrate cGMP-PDEs, *D. rerio* XP_697567 and *X. tropicalis* PDE5a, were not predicted to undergo prenylation using this algorithm (Table 1).

In order to gain insight into the importance of the C*aa*X-box for the prenylation of *Dm*PDE5/6, the putative prenylated cysteine 1128 was mutated to the conservative serine (C1128S). Radio-labelling experiments allowed us to demonstrate post-translational isoprenylation of *Dm*PDE5/6 *in vivo*. Incubation of cells with tritiated mevalonic acid (^{3}[H] MVA), the precursor to isoprenyl pyrophosphate, has been shown to specifically label prenylated proteins [41]. To increase the sensitivity of labelling, the synthesis of iso-prenyl groups from endogenous mevaldate was inhibited by the addition of mevinolin, a 3-Hydroxy-3-methylglutaryl-CoA reductase (HMG-CoA) inhibitor, prior to the addition of [^{3}H] MVA [41]. The Sf9 cell expression system has previously been shown to result in high levels of correctly modified retinal PDE6 subunits [18] and was used here to produce sufficient V5-tagged *Dm*PDE5/6 and C1128S-*Dm*PDE5/6 protein for labelling experiments (Figure 2A).

Western analysis of cell lysates prepared from *Dm*PDE5/6 or C1128S-*Dm*PDE5/6 infected Sf9 cells (pre-treated with mevinolin, and labelled with [^{3}H] MVA) with anti-V5 antibody shows that *Dm*PDE5/6 and C1128S-*Dm*PDE5/6 constructs are expressed at the anticipated size, 130 kDa (Figure 2A, lanes 1 and 2). Immunoprecipitation of cell lysates with anti-*Dm*PDE5/6 antibody [25] increases the amount of *Dm*PDE5/6 and C1128S-*Dm*PDE5/6 proteins (Figure 2A, lanes 4 and 5). Control (uninfected) cell lysates show no immunoreactive species on the Western blot (Figure 2A, lanes 3 and 6).

Corresponding results from SDS-PAGE and autofluorograph analysis (Figure 2B) shows the presence of radio-labelled protein of 130 kDa corresponding to *Dm*PDE5/6 (Figure 2B, lane 1) but not to C1128S-*Dm*PDE5/6 (Figure 2B, lane 2). No 130 kDa protein is detected in control cell extract although there is labelling of endogenous 30 and 60 kDa proteins (Figure 2B, lane 3). Immunoprecipitation of *Dm*PDE5/6 amplifies the signal compared to total lysate and confirms that *Dm*PDE5/6 is radio-labelled with MVA (Figure 2B, lane 4); MVA is not incorporated into C112S-*Dm*PDE5/6-expressing cells or control, uninfected cells (Figure 2B, lanes 5 and 6). Taken together, these results show that *Dm*PDE5/6 undergoes post-translational processing, via the attachment of an isoprenyl group at cysteine 1128 of the C-terminal C*aa*X-box.

Catalytic properties of *Dm*PDE5/6 and the prenylation-deficient C1128S-*Dm*PDE5/6

Both *Dm*PDE5/6 and C1128S-*Dm*PDE5/6 produced by expression in Sf9 cells display similar K_m values for cGMP hydrolysis (C1128S-*Dm*PDE5/6: 35.4 ± 1.2 µM vs *Dm*PDE5/6: 28.1 ± 1.4 µM) (Figure 2C). However, *Dm*PDE5/6 was found to have a relative V_{max} for cGMP hydrolysis approximately 2.2 times greater than that of C1128S-*Dm*PDE5/6 (Figure 2C).

Disruption of prenylation alters sub-cellular distribution of *Dm*PDE5/6 and Ras85D in S2 cells

In order to investigate potential alterations in the sub-cellular localisation of *Dm*PDE5/6 upon ablation of prenylation, V5 epitope-tagged *Dm*PDE5/6 and C1128S-*Dm*PDE5/6 constructs were transfected into *Drosophila* S2 cells. Wild-type *Dm*PDE5/6 is localised to the plasma membrane (Figure 3A). In contrast to this, C1128S-*Dm*PDE5/6 is distributed throughout the cytoplasm (Figure 3B). In order to determine if the altered distribution was due to removal of prenylation rather than simply mutation of Cys1128 per se, we treated S2 cells expressing wild-type *Dm*PDE5/6 with the geranylgeranyl transferase inhibitor 286 (GGTI-286) (1 µM) [42]. This resulted in re-distribution of *Dm*PDE5/6 throughout the cytoplasm (Figure 3C), indicating that prenylation is required for plasma membrane targeting in S2 cells.

The sub-cellular localisation of *Dm*PDE5/6 and C1128S-*Dm*PDE5/6 was also assessed by sub-cellular fractionation. Lysed S2 cells were separated into cytosolic and particulate fractions using centrifugation, followed by detection of *Dm*PDE5/6 through western blotting. *Dm*PDE5/6 was found predominantly in the particulate P15 fraction (Inset, Figure 3A). By contrast, prenyl-deficient C1128S-*Dm*PDE5/6 was found predominantly in the soluble S15 fraction (Inset, Figure 3B). Consistent with confocal immunohistochemical analyses, treatment of transfected S2 cells with GGTI-286 resulted in wild-type *Dm*PDE5/6, now being predominantly localised in the S15 fraction (Inset, Figure 3C). Two bands corresponding to *Dm*PDE5/6 are present in the soluble fraction in Figure 3B and 3C. The lower apparent molecular weight species may represent proteolytic fragments of non-prenylated *Dm*PDE5/6. Alternatively, the different bands may correspond to distinct phosphorylation states of the enzyme.

To confirm that the *Drosophila* S2 cell line is a useful system to analyse the sub-cellular localisation of prenylated proteins, we expressed GFP-tagged *Drosophila* Ras85D, a protein known to undergo lipid modification [43, 44]. Indeed, in all mammalian Ras isoforms, mutation of the putative prenylated cysteine to serine has been shown to prevent the attachment of the isoprenyl group. *Drosophila* Ras85D encodes a C-terminal C*aa*X-box ending in leucine, with a proximal polybasic region (Figure 1A), suggesting that *Drosophila* Ras is a canonical prenylated protein. Confocal analysis shows that GFP-tagged *Drosophila* Ras localises to the plasma membrane with staining of intracellular vesicles and fainter staining of the peri-nuclear region when expressed in *Drosophila* S2 cells (Figure 3D). Furthermore, treatment of GFP-Ras85D expressing cells with 1 μM GGTI-286 resulted in re-distribution of GFP-Ras85D throughout the cytoplasm (Figure 3E). These data provide strong evidence that Ras85D undergoes prenylation in S2 cells and that pharmacological inhibition of this process alters its sub-cellular localisation. Furthermore, this suggests that *Drosophila* S2 cells constitute a useful model for studies of prenylated proteins.

Fractionation experiments confirmed the redistribution of Ras85D in S2 cells after GGTI-286 treatment. GFP-Ras85D is evenly distributed between the insoluble and soluble fractions (Inset, Figure 3D). However, pre-treatment of S2 cells with GGTI-286 completely re-localises Ras85D to the soluble S15 fraction (Inset, Figure 3E).

_Dm_PrBP/δ modulates localisation of _Dm_PDE5/6 in _Drosophila_

Given that retinal PDE6 interacts with PrBP/δ, and that *Dm*PDE5/6 does undergo prenylation *in vivo*, we investigated the existence of a PrBP/δ homologue in *Drosophila*; and the possibility that *Dm*PDE5/6 might interact with *Dm*PrBP/δ. *Dm*PrBP/δ is a polypeptide of 151 amino acids, encoded by gene *CG9296* (http://flybase.bio.indiana.edu/reports/FBgn0032059.html). Alignment with mammalian prenyl-binding proteins shows that the *CG9296* gene product is highly similar to both human and mouse PrBP/δ, with 61% identity and 78% similarity over the entire polypeptide sequence, to human PrBP/δ [20]. When expressed in S2 cells, *Dm*PrBP/δ is targeted predominantly to the nucleus with less intense staining in the cytoplasm (Figure 4A). Fractionation followed by western blotting shows that *Dm*PrBP/δ is predominantly soluble (Inset Figure 4A). To determine if *Dm*PDE5/6 and *Dm*PrBP/δ interact *in vivo*, GFP-tagged *Dm*PDE5/6 and V5-tagged *Dm*PrBP/δ were transfected into S2 cells and their sub-cellular localisation was ascertained by confocal microscopy. Strikingly, when *Dm*PDE5/6 is co-transfected with *Dm*PrBP/δ, the localisation of *Dm*PDE5/6 is altered from the plasma membrane to predominantly intracellular (compare Figure 3A with Figure 4Bi). Indeed, in co-transfection studies the sub-cellular location of *Dm*PDE5/6 now coincides with that of *Dm*PrBP/δ (Figure 4Biii), suggesting that *Dm*PDE5/6 has been sequestered to *Dm*PrBP/δ. Although, these data suggest that *Dm*PrBP/δ provides the dominant intracellular localisation signal, it seems that *Dm*PDE5/6 is not without effect on the localisation of *Dm*PrBP/δ. Thus, in this regard, the nuclear localisation of *Dm*PrBP/δ appears to be compromised when it is co-expressed with *Dm*PDE5/6 compared to when it is expressed alone (contrast Figure 4Bii to figure 4A).

In order to confirm that *Dm*PDE5/6 and *Dm*PrBP/δ can exist in the same complex, co-immunoprecipitation was performed. *Dm*PDE5/6 and *Dm*PrBP/δ were co-transfected into S2 cells and

*Dm*PDE5/6 was immunoprecipitated with a poly-clonal *Dm*PDE5/6 antibody [25]. Western blotting of the immunoprecipitates confirmed that *Dm*PrBP/δ interacts with *Dm*PDE5/6 (Figure 4C).

To further confirm that interaction with *Dm*PrBP/δ altered *Dm*PDE5/6 intracellular localisation, sub-cellular fractionation was undertaken. S2 cells were transfected with either V5-tagged *Dm*PDE5/6 or V5-tagged *Dm*PrBP/δ alone or co-transfected with both proteins, lysed and then separated using differential centrifugation (Figure 5A). The collected fractions were then analysed by western blotting. When expressed alone, *Dm*PDE5/6 was found predominantly in the particulate P1 fraction (Figure 5B), whereas *Dm*PrBP/δ expressed alone resided mainly in the soluble S100 fraction (Figure 5C). In contrast to this, when co-expressed with *Dm*PrBP/δ, *Dm*PDE5/6 occurred mainly in the microsomal P100 fraction (Figure 4D, 130 kDa species). Consistent with the confocal immunohistochemical studies, *Dm*PrBP/δ showed a change in localisation when co-expressed with *Dm*PDE5/6, becoming evenly distributed between the P1, P100 and S100 fractions (Figure 5D, 22 kDa species).

Localisation of C1128S-*Dm*PDE5/6 is disrupted *in vivo*

In order to gain insight into the role of prenylated *Dm*PDE5/6 *in vivo*, the *Drosophila* Malpighian (renal) tubules were utilised as an organotypic screen for *Dm*PDE5/6 function. Previous work demonstrated that *Dm*PDE5/6 is endogenously expressed in tubules [28]. Furthermore, generation of transgenic flies expressing N-terminal GFP-tagged *Dm*PDE5/6 showed that *Dm*PDE5/6 is localised to the apical membrane of principal cells in tubules [28].

In this study, a UAS transgenic line was generated (GFP:C1128S-*Dm*PDE5/6), which allowed targeted expression of GFP-tagged, prenylation-deficient C1128S-*Dm*PDE5/6 in specific cell-types via GAL4 enhancer-trap drivers. Specific expression of GFP-tagged C1128S-*Dm*PDE5/6 in tubule principal cells is effectively achieved using the c42 GAL4 driver [35, 36]. In c42/GFP: C1128S-*Dm*PDE5/6 tubules, staining is mostly observed in the cytoplasm (Figure 6A) compared to GFP:*Dm*PDE5/6 staining, which is located in the apical membrane (Figure 6B and [28]), as indicated by co-localisation with the apical membrane marker, F-actin [33]. However, it is also apparent that a fraction of C1128S-*Dm*PDE5/6 is able to associate with the apical membrane (Fig. 6A). This is supported by fractionation studies (Figure 3), where ablation of prenylation via the C1128S mutation does not completely remove *Dm*PDE5/6 from the membrane to the cytosolic fraction of S2 cells. These data indicate that whilst prenylation provides a major membrane targeting signal there are undoubtedly additional, independent signals that are involved in driving the specific localisation of *Dm*PDE5/6 to the apical membrane.

C1128S-*Dm*PDE5/6 retains biological activity

Tubules expressing C1128S-*Dm*PDE5/6 in the principal cells have significantly increased cGMP-PDE activity compared to control tubules, showing that the transgene is an active cG-PDE *in vivo* (Figure 6C). cGMP-PDE activity is significantly reduced compared to that observed with the transgene encoding wild-type GFP-tagged *Dm*PDE5/6. This may be due to lower expression levels (Figure 6D) and/or the lower V_{max} of C1128S-*Dm*PDE5/6 (Figure 2C) compared to wild-type. Previous work has shown that *Dm*PDE5/6 directly modulates transport of cGMP (efflux) by the tubule [28]: targeted over-expression of *Dm*PDE5/6 inhibits rates of cGMP efflux, while targeted knock-down via RNAi significantly increases cGMP efflux. Expression of C1128S-*Dm*PDE5/6 in principal cells also inhibits cGMP transport rate and ratio (figure 6E and 6F), and to the same extent as that induced by *Dm*PDE5/6 over-expression (figure 6G and 6H).

DISCUSSION

The precise targeting of PDEs to specific sub-cellular locations provides a mechanism for the spatio-temporal control of cyclic nucleotide-mediated signalling events [6, 45, 46] . Prenylation is a lipid post-translational modification that works synergistically with a second signal to promote the membrane-association and, consequently, the biological activity of many proteins [47]. For example, prenylation of

the small GTPase, Ras, is essential for both its membrane-binding and transforming activity [43]. In the mammalian retina, prenylation of the catalytic PDE subunits is required for their binding to rod outer segment membrane and, by inference, effective control of cGMP-mediated visual signal transduction [17]. We show here that *Drosophila melanogaster* PDE5/6 undergoes isoprenyl post-translational modification at its C-terminal C*aa*X-box motif. This is the first non-retinal PDE for which such modification has been demonstrated.

In addition to *Dm*PDE5/6, we have identified a number of putative non-retinal cGMP-PDEs that contain C*aa*X-box motifs and are predicted to undergo prenylation, suggesting that prenylation may be a conserved feature important for their function. Of these, functional data is only available for *Strongylocentrotus purpuratus* PDE5 (suPDE5), a cGMP-PDE involved in sperm motility that is regulated by phosphorylation and pH changes [40]. The presence of a C*aa*X-box motif within suPDE5 suggests prenylation may represent another form of regulation for this enzyme. It will be of interest to determine if suPDE5 is indeed prenylated *in vivo*.

Two putative C*aa*X-box containing PDE sequences, *Xenopus tropicalis* PDE5a and *Danio rerio* XP_697567, have C-terminal regions divergent from that of *Dm*PDE5/6. Analysis by the PrePS prenylation prediction software (http://mendel.imp.ac.at/sat/PrePS/index.html) suggested that neither *X. tropicalis* PDE5a nor *D. rerio* XP_697567 undergo prenylation *in vivo*, due to the presence of unfavourable residues in the +1 to +3 positions after the conserved cysteine. However, we also noted, using the same software, that *D. melanogaster* Ras85D was predicted not to be a substrate for either GGT1 or FT, although our data clearly demonstrate a change in localisation of Ras upon treatment of cells with GGTI-286 (Figure 3D and 3E). This may reflect the relative paucity of published data regarding prenylated *Drosophila* proteins that is available for database compilation, suggesting that there is scope for prenylation *in vivo* of even unfavourable substrates.

Site-directed mutagenesis of the conserved C*aa*X-box cysteine (C1128S) in *Dm*PDE5/6 ablates prenylation and modifies localisation of *Dm*PDE5/6 to the cytoplasm in S2 cells. However, sub-cellular fractionation of S2 cells reveals that a significant proportion of C1128S-*Dm*PDE5/6 remains in the insoluble fraction. In addition to this, C1128S-*Dm*PDE5/6 still shows partial association with the apical membrane when expressed in tubule principal cells. Therefore, removal of *Dm*PDE5/6 prenylation is not sufficient to completely disrupt its localisation. This suggests that whilst prenylation forms an important part of the localisation machinery for *Dm*PDE5/6, additional motifs are required for the fidelity of *Dm*PDE5/6 targeting. Indeed, in many proteins multiple signals are required for efficient targeting to membranes and to signalling complexes[7, 15, 48, 49] This may involve multiple lipid modifications or multiple sites of protein interaction. For example, K-Ras requires both farnesylation and a polybasic region for efficient membrane targeting [15]. However, unlike *Dm*PDE5/6, removal of K-Ras prenylation renders this protein completely soluble [15], suggesting that the targeting sequences for *Dm*PDE5/6 are more complex than for K-Ras. Interestingly, both positive and negative plasma-membrane targeting sequences have been found within the palmitoylated G-protein coupled receptor kinase 6A (GRK6A) [48]. It is plausible that additional sequences facilitating plasma-membrane localisation operate within *Dm*PDE5/6.

The fractionation experiments (figure 3) reveal that two bands corresponding to prenylation-inhibited, wild-type *Dm*PDE5/6 and C1128S-*Dm*PDE5/6 are present in the cytosolic fractions. The lower apparent molecular weight species may represent proteolytic fragments of non-prenylated *Dm*PDE5/6, suggesting that non-prenylated *Dm*PDE5/6 may be more prone to degradation than the wild-type enzyme. Alternatively, the different bands may correspond to distinct phosphorylation states of the *Dm*PDE5/6. This raises the intriguing possibility that prenylation may either protect *Dm*PDE5/6 from phosphorylation by preventing access of a cytosolic kinase or promote phosphorylation by localising *Dm*PDE5/6 to a site where an active kinase resides. Further work will be required to distinguish between these possibilities.

Whilst we could not identify the species of prenyl group that modifies *Dm*PDE5/6, we consider it likely that *Dm*PDE5/6 is modified with a geranylgeranyl group for two reasons. Firstly, the C-terminal amino acid of the *Dm*PDE5/6 C*aa*X-box is leucine, which normally serves as substrate for GGTPase1 [50]. Secondly, we have used the geranylgeranyltransferase-specific inhibitor GGTI-286 in our

experiments, which is highly specific for GGTPase1, and is 15 times more potent at inhibiting GTTPase compared to FTPase *in vivo* [42]. With GGTI-286 we show that the sub-cellular localisation of both Ras85D and *Dm*PDE5/6 is altered upon inhibition of prenyltransferase activity. *Drosophila* possesses homologues of each mammalian prenyltransferase gene [11], therefore, it is likely that the specificity of prenyltransferase inhibitor action will be conserved between mammal and the fly. Furthermore, work investigating the prenylation of *Drosophila* Ras, which also has a leucine at its C-terminus, suggests that this protein undergoes modification with a geranylgeranyl group [44].

Mammalian PrBP/δ binds to the prenylated, C-terminus of the retinal PDE6 catalytic subunits [51], probably serving to sequester the lipid group from the surrounding solvent [52]. We show here that *Dm*PDE5/6 interacts with *Dm*PrBP/δ when these proteins are expressed in S2 cells (Fig. 4). This is the first demonstration of association of a non-retinal PDE with PrBP/δ. Indeed, co-expression of *Dm*PrBP/δ redirects a large proportion of *Dm*PDE5/6 from the plasma membrane to an intracellular location. These data are consistent with the formation of complexes of *Dm*PrBP/δ and *Dm*PDE5/6 where intracellular targeting signals may be compromised in a number of ways. They could be masked, either with the geranylgeranyl group on *Dm*PDE5/6 being bound to *Dm*PrBP/δ or through steric hindrance through protein-protein interaction, which may ablate, compromise or reprogram interactions. Furthermore, if targeting signals remain on each protein then sequestering proteins will serve to compete for the *Dm*PDE5/6-*Dm*PrBP/δ complex, their efficacy being driven by their concentration and relative affinity.

The Malpighian tubule of *Drosophila* transports cGMP from the basolateral hemolymph to the lumen [28]. Over-expression of *Dm*PDE5/6 in the tubule principal cell has been shown to inhibit cGMP transport. Despite the altered sub-cellular localisation of C1128S-*Dm*PDE5/6, over-expression of non-prenylated *Dm*PDE5/6 in principal cells also inhibits cGMP transport. This is likely due to the mass of over-expressed C1128S-*Dm*PDE5/6 in the tubule, enabling a biological response in spite of the altered sub-cellular localisation. Alternatively, residual targeting of C1128S-*Dm*PDE5/6 to the apical membrane may account for the inhibition of cGMP transport in these tubules.

The identification here of the first non-retinal cGMP-PDE to undergo prenylation, and the detection of several cGMP-PDEs with C*aa*X-boxes suggests that prenylation of phosphodiesterases may be more common than previously thought. The molecular characterisation of further putative prenylated cGMP-PDEs will help shed light on the importance of prenylation for cGMP-mediated signal-transduction in non-retinal tissue. Further investigation of *Dm*PDE5/6 function may provide insights into the role of prenylated non-retinal PDEs from other species.

ACKNOWLEDGEMENTS

This work was supported by the UK Biotechnology and Biological Sciences Council (BB/C00633/1), and the UK Medical Research Council (G8604010).

REFERENCES

1 Carlisle Michel, J. J., Dodge, K. L., Wong, W., Mayer, N. C., Langeberg, L. K. and Scott, J. D. (2004) PKA-phosphorylation of PDE4D3 facilitates recruitment of the mAKAP signalling complex. Biochem. J. **381**, 587-592

2 Schlossmann, J., Feil, R. and Hofmann, F. (2003) Signaling through NO and cGMP-dependent protein kinases. Ann. Med. **35**, 21-27

3 Zabel, U., Kleinschnitz, C., Oh, P., Nedvetsky, P., Smolenski, A., Muller, H., Kronich, P., Kugler, P., Walter, U., Schnitzer, J. E. and Schmidt, H. H. (2002) Calcium-dependent membrane association sensitizes soluble guanylyl cyclase to nitric oxide. Nat. Cell Biol. **4**, 307-311

4 Willoughby, D. and Cooper, D. M. (2007) Organization and Ca2+ regulation of adenylyl cyclases in cAMP microdomains. Physiol. Rev. **87**, 965-1010

5 Conti, M. and Beavo, J. (2007) Biochemistry and physiology of cyclic nucleotide phosphodiesterases: essential components in cyclic nucleotide signaling. Ann. Rev. Biochem. **76**, 481-511

6 Baillie, G. S. and Houslay, M. D. (2005) Arrestin times for compartmentalised cAMP signalling and phosphodiesterase-4 enzymes. Curr. Opin. Cell Biol. **17**, 129-134

7 Bolger, G. B., Baillie, G. S., Li, X., Lynch, M. J., Herzyk, P., Mohamed, A., Mitchell, L. H., McCahill, A., Hundsrucker, C., Klussmann, E., Adams, D. R. and Houslay, M. D. (2006) Scanning peptide array analyses identify overlapping binding sites for the signalling scaffold proteins, beta-arrestin and RACK1, in cAMP-specific phosphodiesterase PDE4D5. Biochem. J. **398**, 23-36

8 Perry, S. J., Baillie, G. S., Kohout, T. A., McPhee, I., Magiera, M. M., Ang, K. L., Miller, W. E., McLean, A. J., Conti, M., Houslay, M. D. and Lefkowitz, R. J. (2002) Targeting of cyclic AMP degradation to beta 2-adrenergic receptors by beta-arrestins. Science **298**, 834-836

9 Dodge-Kafka, K. L., Soughayer, J., Pare, G. C., Carlisle Michel, J. J., Langeberg, L. K., Kapiloff, M. S. and Scott, J. D. (2005) The protein kinase A anchoring protein mAKAP coordinates two integrated cAMP effector pathways. Nature **437**, 574-578

10 Dodge, K. L., Khouangsathiene, S., Kapiloff, M. S., Mouton, R., Hill, E. V., Houslay, M. D., Langeberg, L. K. and Scott, J. D. (2001) mAKAP assembles a protein kinase A/PDE4 phosphodiesterase cAMP signaling module. Embo J. **20**, 1921-1930

11 Maurer-Stroh, S., Washietl, S. and Eisenhaber, F. (2003) Protein prenyltransferases. Genome Biol. **4**, 212

12 Resh, M. D. (2004) Membrane targeting of lipid modified signal transduction proteins. Subcell. Biochem. **37**, 217-232

13 Willumsen, B. M., Christensen, A., Hubbert, N. L., Papageorge, A. G. and Lowy, D. R. (1984) The p21 ras C-terminus is required for transformation and membrane association. Nature **310**, 583-586

14 Maurer-Stroh, S. and Eisenhaber, F. (2005) Refinement and prediction of protein prenylation motifs. Genome Biol. **6**, R55

15 Hancock, J. F., Paterson, H. and Marshall, C. J. (1990) A polybasic domain or palmitoylation is required in addition to the CAAX motif to localize p21ras to the plasma membrane. Cell **63**, 133-139

16 Anant, J. S., Ong, O. C., Xie, H. Y., Clarke, S., O'Brien, P. J. and Fung, B. K. (1992) In vivo differential prenylation of retinal cyclic GMP phosphodiesterase catalytic subunits. J Biol. Chem. **267**, 687-690

17 Qin, N., Pittler, S. J. and Baehr, W. (1992) In vitro isoprenylation and membrane association of mouse rod photoreceptor cGMP phosphodiesterase alpha and beta subunits expressed in bacteria. J. Biol. Chem. **267**, 8458-8463

18 Qin, N. and Baehr, W. (1994) Expression and mutagenesis of mouse rod photoreceptor cGMP phosphodiesterase. J. Biol. Chem. **269**, 3265-3271

19 Norton, A. W., Hosier, S., Terew, J. M., Li, N., Dhingra, A., Vardi, N., Baehr, W. and Cote, R. H. (2005) Evaluation of the 17-kDa prenyl-binding protein as a regulatory protein for phototransduction in retinal photoreceptors. J. Biol. Chem. **280**, 1248-1256

20 Nancy, V., Callebaut, I., El Marjou, A. and de Gunzburg, J. (2002) The delta subunit of retinal rod cGMP phosphodiesterase regulates the membrane association of Ras and Rap GTPases. J. Biol. Chem. **277**, 15076-15084

21 Gillespie, P. G., Prusti, R. K., Apel, E. D. and Beavo, J. A. (1989) A soluble form of bovine rod photoreceptor phosphodiesterase has a novel 15-kDa subunit. J. Biol. Chem. **264**, 12187-12193

22 Zhang, H., Li, S., Doan, T., Rieke, F., Detwiler, P. B., Frederick, J. M. and Baehr, W. (2007) Deletion of PrBP/delta impedes transport of GRK1 and PDE6 catalytic subunits to photoreceptor outer segments. Proc. Natl. Acad. Sci. U S A **104**, 8857-8862

23 Francis, S. H. and Corbin, J. D. (2005) Phosphodiesterase-5 inhibition: the molecular biology of erectile function and dysfunction. Urol. Clin. North Am. **32**, 419-429, vi

24 Cote, R. H. (2004) Characteristics of photoreceptor PDE (PDE6): similarities and differences to PDE5. Int. J. Impot. Res. **16 Suppl 1**, S28-33

25 Day, J. P., Dow, J. A., Houslay, M. D. and Davies, S. A. (2005) Cyclic nucleotide phosphodiesterases in Drosophila melanogaster. Biochem. J. **388**, 333-342

26 Lugnier, C., Schoeffter, P., Le Bec, A., Strouthou, E. and Stoclet, J. C. (1986) Selective inhibition of cyclic nucleotide phosphodiesterases of human, bovine and rat aorta. Biochem. Pharmacol. **35**, 1743-1751

27 Boolell, M., Allen, M. J., Ballard, S. A., Gepi-Attee, S., Muirhead, G. J., Naylor, A. M., Osterloh, I. H. and Gingell, C. (1996) Sildenafil: an orally active type 5 cyclic GMP-specific phosphodiesterase inhibitor for the treatment of penile erectile dysfunction. Int. J. Impot. Res. **8**, 47-52

28 Day, J. P., Houslay, M. D. and Davies, S. A. (2006) A novel role for a Drosophila homologue of cGMP-specific phosphodiesterase in the active transport of cGMP. Biochem. J. **393**, 481-488

29 Brand, A. H. and Perrimon, N. (1993) Targeted gene expression as a means of altering cell fates and generating dominant phenotypes. Development **118**, 401-415

30 Radford, J. C., Davies, S. A. and Dow, J. A. (2002) Systematic G-protein-coupled receptor analysis in Drosophila melanogaster identifies a leucokinin receptor with novel roles. J. Biol. Chem. **277**, 38810-38817

31 MacPherson, M. R., Lohmann, S. M. and Davies, S. A. (2004) Analysis of Drosophila cGMP-dependent protein kinases and assessment of their in vivo roles by targetted expression in a renal transporting epithelium. J. Biol. Chem.

32 MacPherson, M. R., Pollock, V. P., Broderick, K. E., Kean, L., O'Connell, F. C., Dow, J. A. and Davies, S. A. (2001) Model organisms: new insights into ion channel and transporter function. L-type calcium channels regulate epithelial fluid transport in Drosophila melanogaster. Am. J. Physiol. Cell Physiol. **280**, C394-407

33 Denholm, B., Sudarsan, V., Pasalodos-Sanchez, S., Artero, R., Lawrence, P., Maddrell, S., Baylies, M. and Skaer, H. (2003) Dual origin of the renal tubules in Drosophila: mesodermal cells integrate and polarize to establish secretory function. Curr. Biol. **13**, 1052-1057

34 Parker, L., Gross, S. and Alphey, L. (2001) Vectors for the expression of tagged proteins in Drosophila. Biotechniques **31**, 1280-1282, 1284, 1286

35 Broderick, K. E., Kean, L., Dow, J. A. T., Pyne, N. J. and Davies, S. A. (2004) Ectopic expression of bovine type 5 phosphodiesterase confers a renal phenotype in Drosophila. J. Biol. Chem. **279**, 8159-8168

36 Rosay, P., Davies, S. A., Yu, Y., Sozen, A., Kaiser, K. and Dow, J. A. (1997) Cell-type specific calcium signalling in a Drosophila epithelium. J. Cell. Sci. **110 (Pt 15)**, 1683-1692

37 MacPherson, M. R., Broderick, K. E., Graham, S., Day, J. P., Houslay, M. D., Dow, J. A. and Davies, S. A. (2004) The dg2 (for) gene confers a renal phenotype in Drosophila by modulation of cGMP-specific phosphodiesterase. J. Exp. Biol. **207**, 2769-2776

38 Torrie, L. S., Radford, J. C., Southall, T. D., Kean, L., Dinsmore, A. J., Davies, S. A. and Dow, J. A. (2004) Resolution of the insect ouabain paradox. Proc. Natl. Acad. Sci. U S A

39 Weber, B., Riess, O., Hutchinson, G., Collins, C., Lin, B. Y., Kowbel, D., Andrew, S., Schappert, K. and Hayden, M. R. (1991) Genomic organization and complete sequence of the human gene encoding the beta-subunit of the cGMP phosphodiesterase and its localisation to 4p 16.3. Nucleic Acids Res. **19**, 6263-6268

40 Su, Y. H. and Vacquier, V. D. (2006) Cyclic GMP-specific phosphodiesterase-5 regulates motility of sea urchin spermatozoa. Mol. Biol. Cell **17**, 114-121

41 Khosravi-Far, R. and Der, C. J. (1995) Prenylation Analysis of Bacterially Expressed and Insect Cell-Expressed Ras and Ras-Related Proteins. In Small GTPases and Their Regulators (Balch, W. E., Der, C. J. and Hall, A., eds.), pp. 46-59, Academic Press, London

42 Lerner, E. C., Qian, Y., Hamilton, A. D. and Sebti, S. M. (1995) Disruption of oncogenic K-Ras4B processing and signaling by a potent geranylgeranyltransferase I inhibitor. J. Biol. Chem. **270**, 26770-26773

43 Hancock, J. F., Magee, A. I., Childs, J. E. and Marshall, C. J. (1989) All ras proteins are polyisoprenylated but only some are palmitoylated. Cell **57**, 1167-1177

44 Kauffmann, R. C., Qian, Y., Vogt, A., Sebti, S. M., Hamilton, A. D. and Carthew, R. W. (1995) Activated Drosophila Ras1 is selectively suppressed by isoprenyl transferase inhibitors. Proc. Natl. Acad. Sci. U S A **92**, 10919-10923

45 Houslay, M. D. and Adams, D. R. (2003) PDE4 cAMP phosphodiesterases: modular enzymes that orchestrate signalling cross-talk, desensitization and compartmentalization. Biochem. J. **370**, 1-18

46 Houslay, M. D., Baillie, G. S. and Maurice, D. H. (2007) cAMP-Specific phosphodiesterase-4 enzymes in the cardiovascular system: a molecular toolbox for generating compartmentalized cAMP signaling. Circ. Res. **100**, 950-966

47 Resh, M. D. (2006) Trafficking and signaling by fatty-acylated and prenylated proteins. Nat. Chem. Biol. **2**, 584-590

48 Jiang, X., Benovic, J. L. and Wedegaertner, P. B. (2007) Plasma membrane and nuclear localization of G protein coupled receptor kinase 6A. Mol. Biol. Cell **18**, 2960-2969

49 Smith, K. J., Baillie, G. S., Hyde, E. I., Li, X., Houslay, T. M., McCahill, A., Dunlop, A. J., Bolger, G. B., Klussmann, E., Adams, D. R. and Houslay, M. D. (2007) (1)H NMR structural and functional characterisation of a cAMP-specific phosphodiesterase-4D5 (PDE4D5) N-terminal region peptide that disrupts PDE4D5 interaction with the signalling scaffold proteins, betaarrestin and RACK1. Cell. Signal. **19**, 2612-2624

50 Moores, S. L., Schaber, M. D., Mosser, S. D., Rands, E., O'Hara, M. B., Garsky, V. M., Marshall, M. S., Pompliano, D. L. and Gibbs, J. B. (1991) Sequence dependence of protein isoprenylation. J. Biol. Chem. **266**, 14603-14610

51 Cook, T. A., Ghomashchi, F., Gelb, M. H., Florio, S. K. and Beavo, J. A. (2000) Binding of the delta subunit to rod phosphodiesterase catalytic subunits requires methylated, prenylated C-termini of the catalytic subunits. Biochemistry **39**, 13516-13523

52 Hanzal-Bayer, M., Renault, L., Roversi, P., Wittinghofer, A. and Hillig, R. C. (2002) The complex of Arl2-GTP and PDE delta: from structure to function. Embo J. **21**, 2095-2106

FIGURE LEGENDS

Table 1. Sequence identity (similarity) between cGMP-PDEs with putative prenylation motifs and Human PDE5A1, Human PDE11A4 and *Dm*PDE5/6.

Fig. 1. C*aa*X-box prenylation motifs occur in non-retinal cGMP-PDEs from non-mammalian classes. cGMP-PDE sequences containing putative C*aa*X-box prenylation motifs were identified using BLAST-searching of the non-redundant protein database with *Dm*PDE5/6 as the query sequence. Protein sequences were aligned and sequence similarity tree was generated using ClustalW (**http://www.ebi.ac.uk/Tools/clustalw/**) [46]. **A**. Alignment of the C-terminal 25 amino acids of C*aa*X-box cGMP-PDEs (highlighted in red) and *Dm*Ras85D, showing conserved C*aa*X-box cysteine residue, shaded black. **B**. Sequence similarity tree of cGMP-PDEs with C*aa*X-box prenylation motifs (highlighted in red) with human PDE5A1, human PDE11A4 and human retinal PDE catalytic subunits as reference sequences.

Fig. 2. *Dm*PDE5/6 is prenylated at a C-terminal C*aa*X-box. **A**. Western analysis of [^{3}H] MVA labelled Sf9 cells expressing wild-type *Dm*PDE5/6 (WT), C1128S-*Dm*PDE5/6 (CS) or uninfected control cells (CON). Either 10 µg of total lysate (lanes 1-3) or *Dm*PDE5/6 immunoprecipitated with a rabbit polyclonal anti-*Dm*PDE5/6 antibody, [14] (lanes 4-6) were analysed. **B**. Fluorograph of samples shown in panel A, lanes denoted as in A. Positive bands for *Dm*PDE5/6 and C1128S-*Dm*PDE5/6 are observed at 130 kDa. **C**. Comparison of the Michaelis-Menton plots for cG-PDE activity of *Dm*PDE5/6 and C1128S-*Dm*PDE5/6 expressed in Sf9 cells. Equal relative amounts, as ascertained by western blotting, of either *Dm*PDE5/6 (triangles) or C1128S-*Dm*PDE5/6 (squares) were assayed for cGMP-PDE activity, nmol cGMP/mg/min ± S.E.M, $N = 3$.

Fig. 3. Plasma membrane association of *Dm*PDE5/6 and Ras85D in S2 cells is affected by prenylation
A, B, D: Plasmids encoding wild-type *Dm*PDE5/6 (A), C1128S mutation of *Dm*PDE5/6 (B) and GFP-tagged Ras85D (D) were expressed in S2 cells. *Dm*PDE5/6 and C1128S-*Dm*PDE5/6 were localised with anti-V5 antibody using confocal microscopy. **C, E.** Transfected cells were also treated with the prenylation inhibitor GGTI-286, transfected with *Dm*PDE5/6 (C) and GFP-tagged Ras85D (E) and the expressed protein visualised accordingly. Control (untransfected) cells did not show staining with anti-V5 antibody (not shown). In all panels, single cells are shown in which cell nuclei were stained with DAPI (blue). Scale bars in all images correspond to 5 µm.
A-E, Insets: Cell fractionation and Western blotting of *Dm*PDE5/6 and C1128S-*Dm*PDE5/6 using anti-V5 antibody (130 kDa) and of GFP:Ras85D (50 kDa) using anti-GFP antibody. Fractions assayed for presence of expressed protein were: P15 and S15 as described in Materials and Methods.

Fig. 4. *Dm*PDE5/6 interacts with *Dm*PrBP/δ
A. Localisation of C-terminal V5-tagged *Dm*PrBP/δ expressed in S2 cells **B**. S2 cells were transiently co-transfected with V5-tagged *Dm*PrBP/δ (red) and GFP:*Dm*PDE5/6 (green), stained with anti-V5 antibody and DAPI (blue) and viewed by confocal microscopy. **i**. GFP:*Dm*PDE5/6; **ii**. *Dm*PrBP/δ; **iii.** Merge of GFP:*Dm*PDE5/6 with *Dm*PrBP/δ showing co-localisation (yellow). **C**. Co-immunoprecipitation of *Dm*PDE5/6 with *Dm*PrBP/δ. S2 cells were transiently transfected with *Dm*PDE5/6 and *Dm*PrBP/δ, or with *Dm*PrBP/δ on its own. Cell lysates were subjected to western blotting to confirm expression of constructs (bottom two panels) and *Dm*PDE5/6 was immunoprecipitated using an anti-*Dm*PDE5/6 poly clonal antibody. Western analysis confirms *Dm*PDE6 was precipitated (second panel) whereas top panel shows that *Dm*PrBP/δ co-precipitates with *Dm*PDE5/6.

Fig. 5. Altered sub-cellular localisation of *Dm*PDE5/6 in response to *Dm*PrBP/δ expression
A. S2 cells were transfected with V5-tagged *Dm*PDE5/6 and/or *Dm*PrBP/δ, lysed and separated into sub-cellular fractions using variable centrifugation. **B**. Western blot of fractionated V5-tagged *Dm*PDE5/6. **C**. Western blot of fractionated V5-tagged *Dm*PrBP/δ. **D**. Western blot of fractionated *Dm*PDE5/6 co-expressed with *Dm*PrBP/δ.

Fig. 6. Mis-localisation of C1128S-*Dm*PDE5/6 in a polarised epithelium.
The transgenic UAS-GFP: C1128S-*Dm*PDE5/6 line was generated and crossed to the principal-cell specific c42 driver. Tubules from adult progeny were dissected, stained for the apical membrane marker F-actin using phalloidin; and counterstained with the nuclear stain DAPI, 4', 6'-diamidino-2-phenylindole hydrochloride. **A.** c42/GFP: C1128S-*Dm*PDE5/6 **B.** for comparison, staining in c42/GFP:*Dm*PDE5/6 transgenic tubules [17] is shown. Scale bars are 10 μm; tubule diameter can be taken as 35 μm. In panels A and B, green fluorescence denotes GFP-tagged C1128S-*Dm*PDE5/6 (A, apical staining indicated by white arrows; cytoplasmic staining indicated by yellow arrow) or GFP-tagged *Dm*PDE5/6 (B, apical staining indicated by white arrows, basolateral staining indicated by blue arrow); F-actin is stained red, and nuclei stained blue. No GFP signal was observed in either parental c42 or UAS tubules (data not shown). **C.** The C1128S-*Dm*PDE5/6 transgene encodes active cG-PDE enzyme in tubules. Measurements of cG-PDE activity in tubules from c42, UAS-GFP: C1128S-*Dm*PDE5/6, c42/UAS-GFP: *Dm*PDE5/6 C1128S are shown. For clarity, data for cG-PDE activity in tubules of UAS-GFP:*Dm*PDE5/6, c42/UAS-GFP:*Dm*PDE5/6 [17] are included. Data are expressed as mean cG-PDE activity, (pmol cGMP/min/mg protein) ± SEM, N=3-6. Significance (compared to parental lines) denoted by *, $p<0.05$, Student's t-test. **D.** Western blot of GFP:C1128S-*Dm*PDE5/6 and GFP:*Dm*PDE5/6 expressed in principal-cells using anti-GFP antibody (top panel). Loading control using anti-γ-tubulin antibody (lower panel). **E.** Rates of cGMP transport for UAS-GFP:C1128S-*Dm*PDE5/6 and c42/UAS-GFP:C1128S-*Dm*PDE5/6 tubules are shown. **F.** cGMP transport ratio, where active transport is defined as a ratio of more than 1, in UAS-GFP:C1128S-*Dm*PDE5/6 and c42/UAS-GFP:C1128S-*Dm*PDE5/6 tubules. **G**. Rates of cGMP transport for UAS-GFP:*Dm*PDE5/6 and c42/UAS-GFP:*Dm*PDE5/6 tubules. **H**. cGMP transport ratios for UAS-GFP:*Dm*PDE5/6 and c42/UAS-GFP:*Dm*PDE5/6 tubules. cGMP transport rate data are expressed as pmol cGMP/min ± SEM, N=12. Transport ratio expressed ± SEM, N=12. Significance denoted by *, $p<0.05$, Student's t-test.

Protein	Percentage identities (similarities) with *Hs*PDE5A1	Percentage identities (similarities) with *Hs*PDE11A4	Percentage identities (similarities) with *Hs*PDE6B	Percentage identities (similarities) with *Dm*PDE5/6	PrePS (http://mendel.imp.univie.ac.at/sat/PrePS) score	
					Farnesyl transferase	Geranylgeranyl transferase 1
D. melanogaster PDE5/6	30 (14)	31 (13)	23 (15)		-0.262	+1.551
D. pseudoobscura GA20950	30 (14)	30 (14)	23 (15)	88 (3)	-0.386	+1.200
A. gambiae AGAP004119	34 (16)	34 (16)	25 (17)	62 (9)	-0.982	+0.260
A. mellifera XP_394107	34 (16)	34 (14)	28 (16)	57 (10)	-0.402	-1.128
T. castaneum XP_967847	36 (14)	36 (15)	29 (18)	55 (11)	-0.720	+2.606
S. purpuratus PDE5	36 (16)	36 (16)	29 (17)	39 (14)	-0.170	-0.776
D. rerio XP_697567	35 (18)	71 (9)	28 (17)	30 (15)	-4.786	-17.436
X. tropicalis PDE5a	75 (9)	33 (18)	28 (20)	31 (13)	-7.757	-20.246

Table 1.

Figure 1

A

```
D. melanogaster PDE5/6          S S S T S S A G G Q M V D K S - - K K R S K L C A L L
D. pseudoobscura GA20950        S S S T S S A G - T V V D K S - - K K R S K L C S L L
A. gambiae AGAP004119           - - G T D Q H H E Q A M S H S P V K K R S K L C M L L
A. mellifera XP_394107          P E D A A K S T K A L I P D R - - K S R N K L C L L I
S. purpuratus PDE5              G S Q M S Q Q C K E A L A A K - - K N K S S L C S V I
T. castaneum XP_967847          - - A P A C Q Q L P P L G H K L K R N K H K L C C I L
D. rerio XP_697567              - - E G S T H G V E P K Q T P V A N Y K E G A C C G H
X. tropicalis PDE5a             - I L A E Q Q E K N L V N G A K - S Q P E V K C N M D
H. sapiens PDE6B                - V A A K K V G T E I C N G G P - A P K S S T C C I L
D. melanogaster Ras85D          - K D K D N K G R R G R K M N K - P N R R F K C K M L
```

B

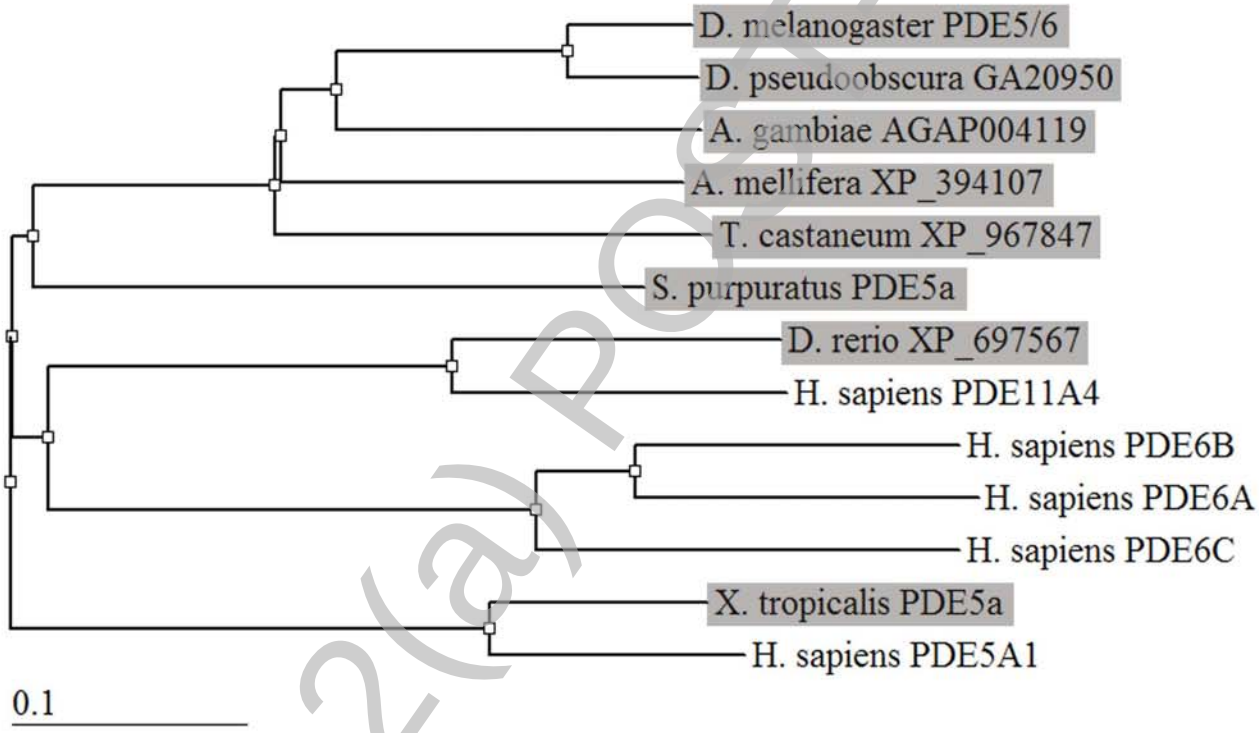

Figure 2

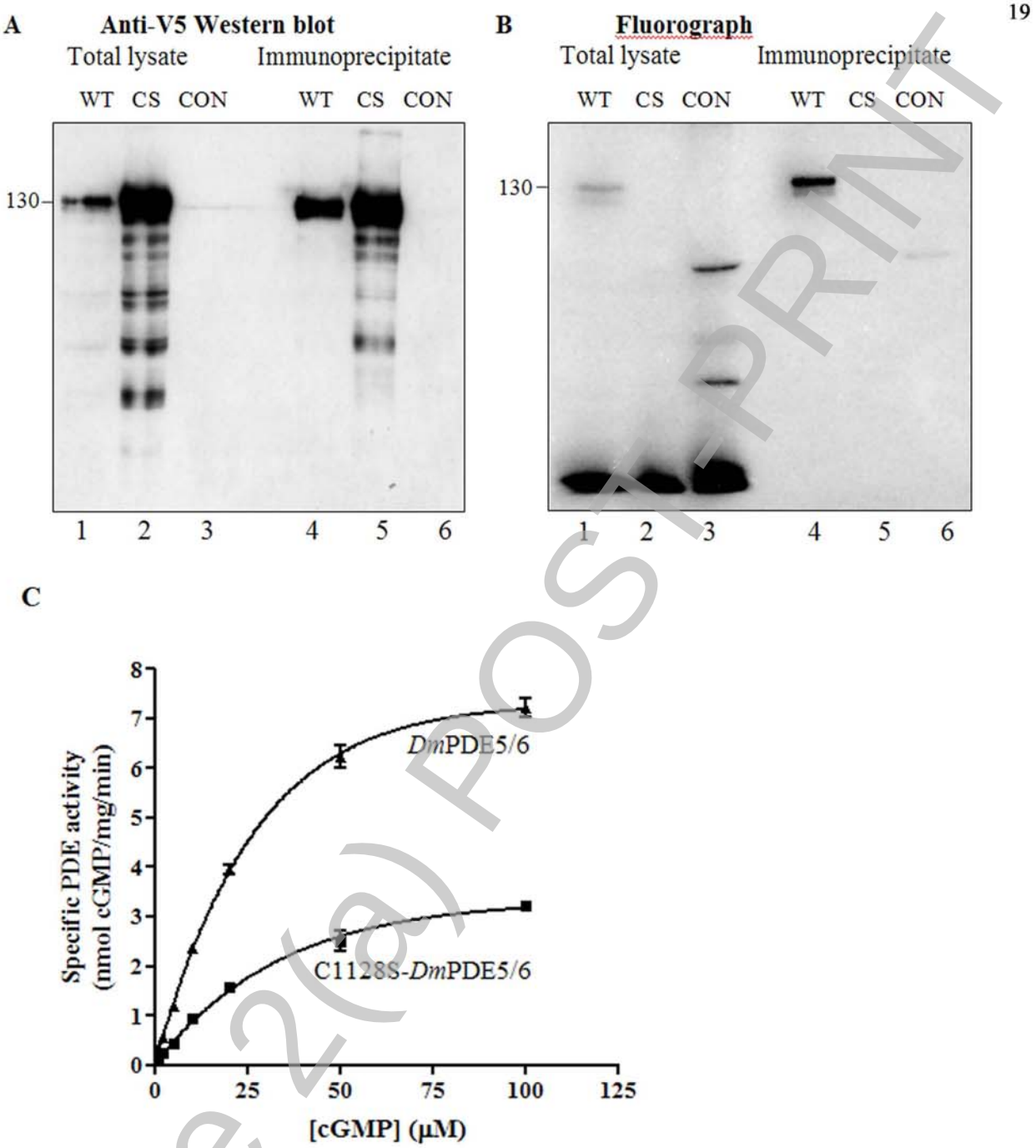

Figure 3

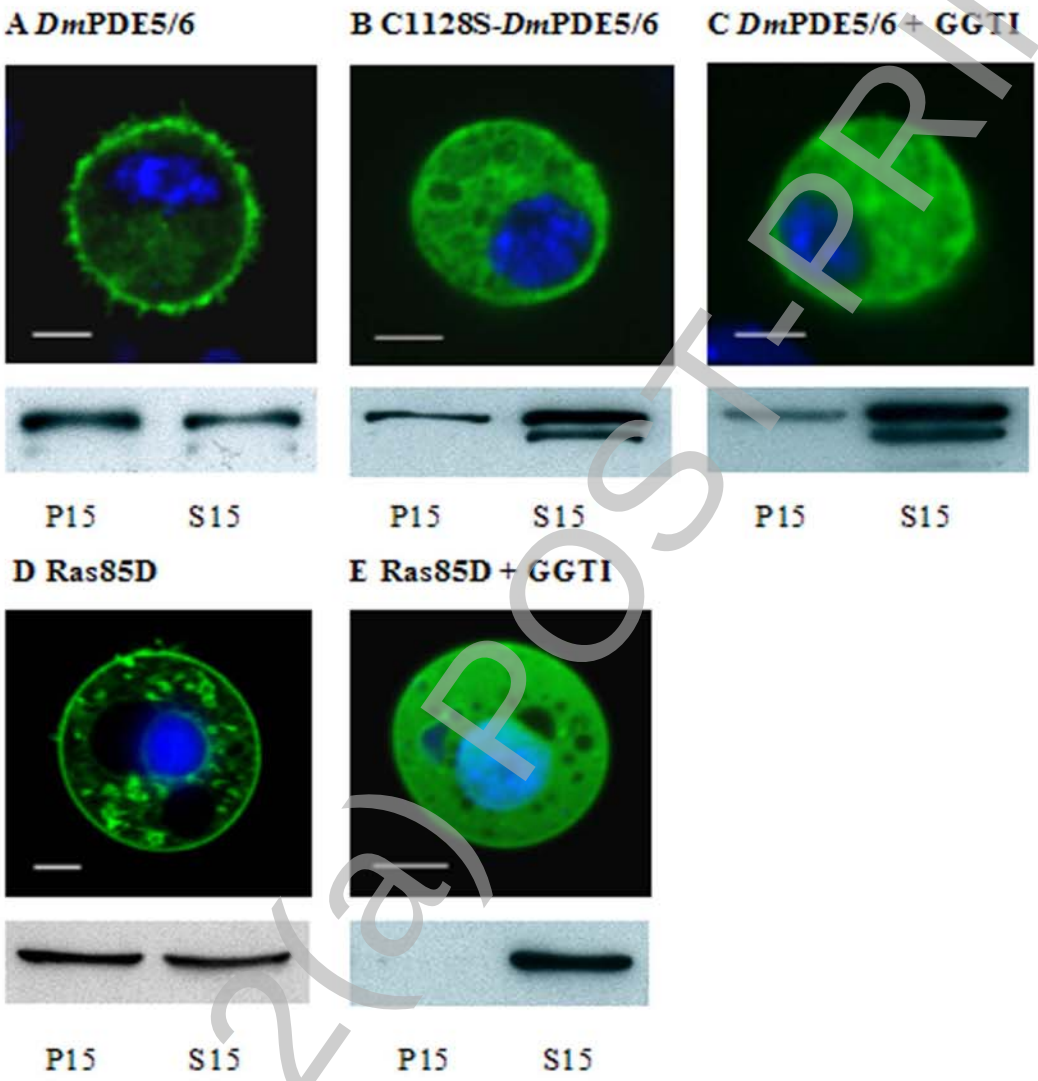

Figure 4

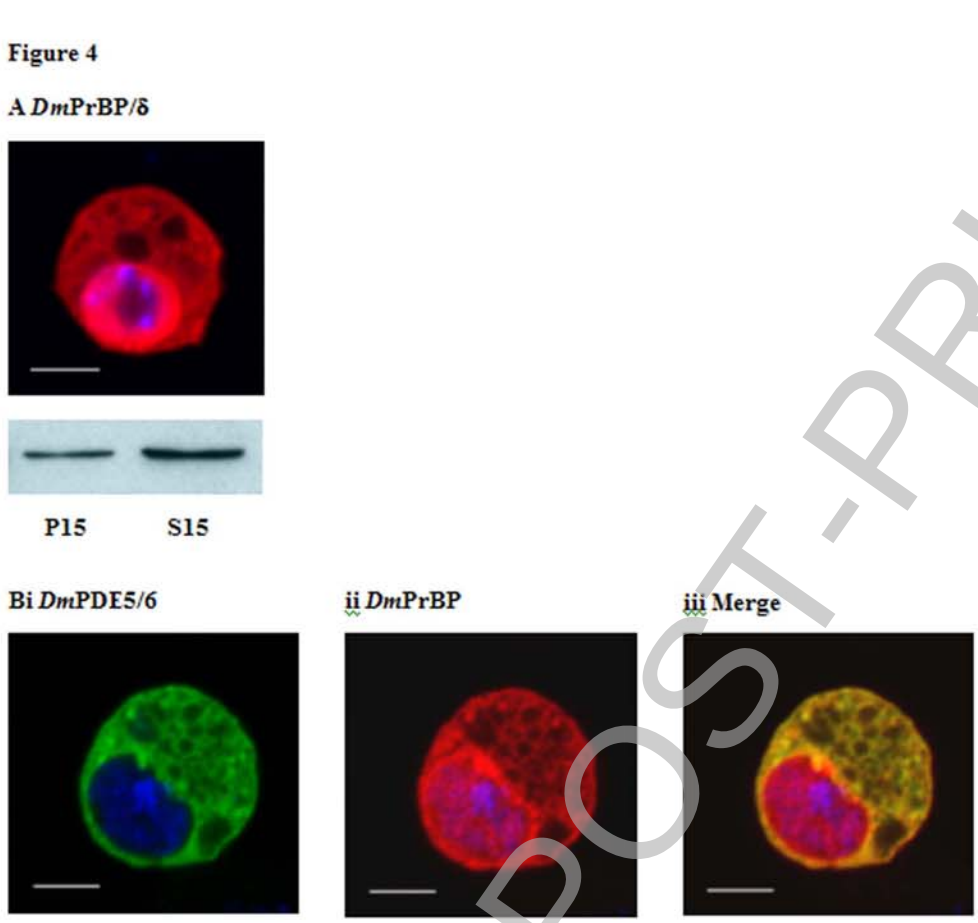

Figure 5

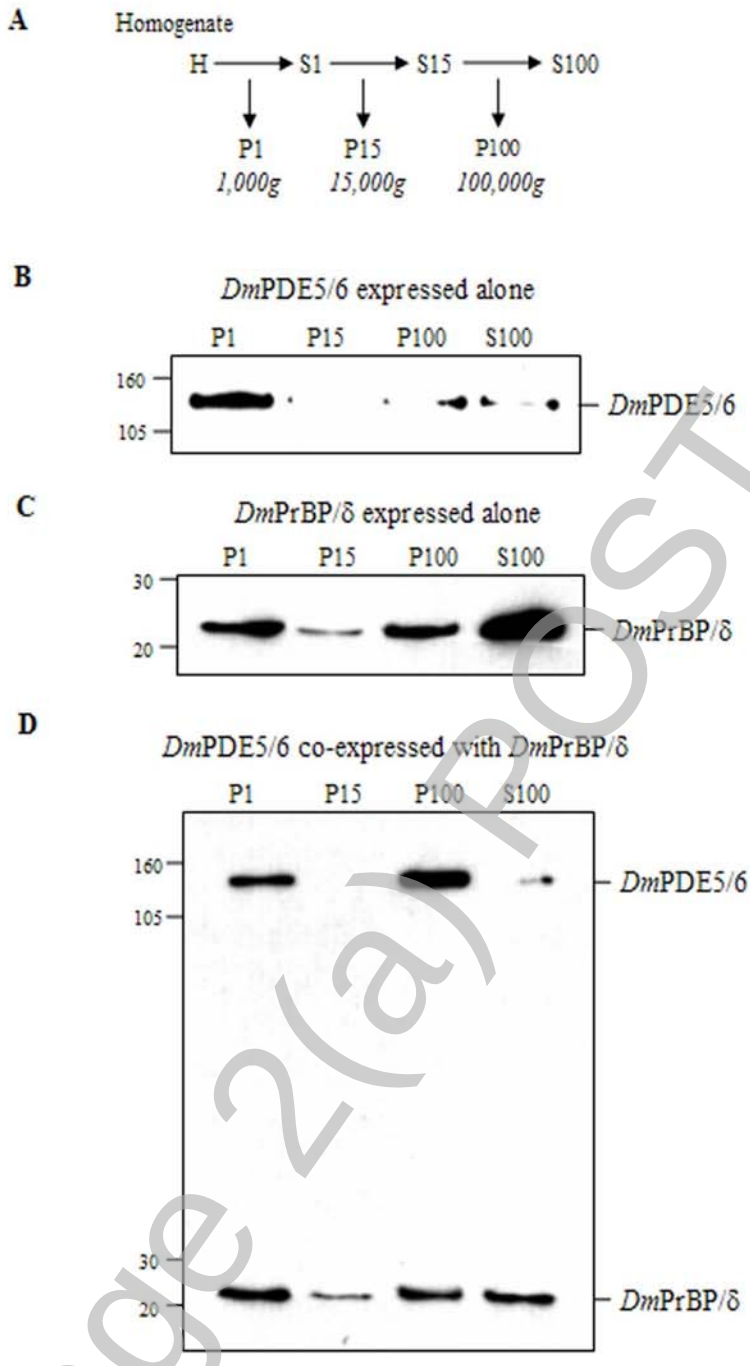

Figure 6

A Targeted GFP:C1128S *Dm*PDE5/6

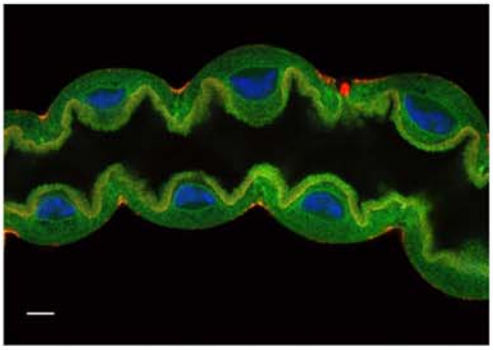

B Targeted GFP :*Dm*PDE5/6

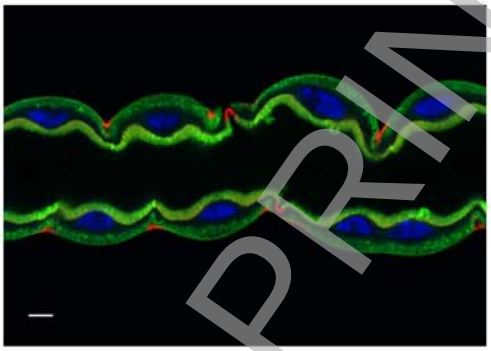

C Tubule cGMP-PDE activity

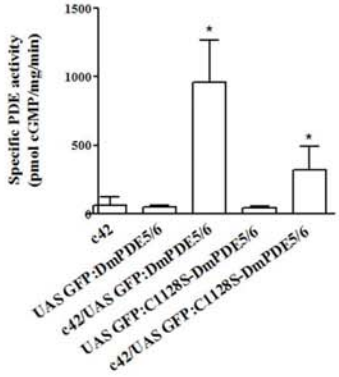

D Western blot of GFP-tagged *Dm*PDE5/6

E cGMP transport rate - C1128S *Dm*PDE5/6

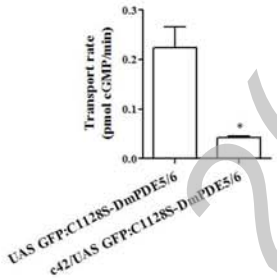

F cGMP transport ratio - C1128S *Dm*PDE5/6

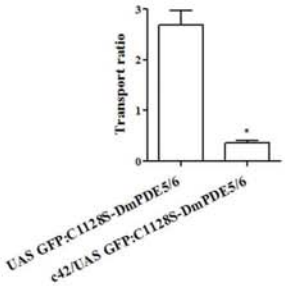

G cGMP transport rate - *Dm*PDE5/6

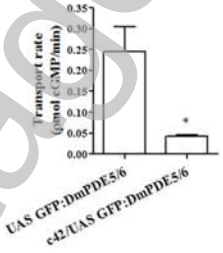

H cGMP transport ratio - *Dm*PDE5/6